forests

MDPI

Article

Eucalyptus-Based Glued Laminated Timber: Evaluation and Prediction of Its Properties by Non-Destructive Techniques

Ramon Ferreira Oliveira [1], Pedro Gutemberg de Alcântara Segundinho [1,*], João Gabriel Missia da Silva [1], Fabricio Gomes Gonçalves [1], Dercílio Junior Verly Lopes [1], Jeferson Pereira Martins Silva [1], Nayara Franzini Lopes [2], Leonor da Cunha Mastela [1], Juarez Benigno Paes [1], Clara Gaspar Fossi de Souza [3], Francisco Antônio Rocco Lahr [3], Maria Alice Romanha Belumat [1], André Luis Christoforo [4] and Caroline Palacio de Araujo [1]

[1] Departament of Forest and Wood Science, Federal University of Espírito Santo, Avenida Governador Lindemberg, Jerônimo Monteiro 29550-000, ES, Brazil; oliveira.r.eim@gmail.com (R.F.O.); j.gabrielmissia@hotmail.com (J.G.M.d.S.); fabricio.goncalves@ufes.br (F.G.G.); dercilioIopes@icloud.com (D.J.V.L.); jefersonsb09@hotmail.com (J.P.M.S.); leonor.mastela@ufes.br (L.d.C.M.); jbp2@uol.com.br (J.B.P.); maralice.romanha@gmail.com (M.A.R.B.); carolinepalacio@yahoo.com.br (C.P.d.A.)

[2] Department of Forest Engineering, Federal University of Viçosa, Avenida P. H. Rolfs, s/n, Viçosa 36570-900, MG, Brazil; nayaraflopes@hotmail.com

[3] São Carlos School of Engineering, University of São Paulo, Avenida Trabalhador São Carlense, 400, Parque Arnold Schimidt, São Carlos 13566-590, SP, Brazil; clara.gaspar@hotmail.com (C.G.F.d.S.); frocco@sc.usp.br (F.A.R.L.)

[4] Department of Civil Engineering, Federal University of São Carlos, Rodovia Washington Luís, km 235, s/n, Jardim Guanabara, São Carlos 13565-905, SP, Brazil; christoforoal@yahoo.com.br

* Correspondence: p_gutemberg2001@yahoo.com.br

Abstract: Eucalyptus-based glued laminated timber (glulam) was produced to determine the feasibility of a non-destructive method (drilling resistance) to predict the properties of structural elements and add value to lower-quality hardwood species. Glulam was manufactured with formaldehyde (Resorcinol), reference condition, and bio-based (Castor oil-based) adhesives in two assembly schemes, the core composed either of two continuous lamellae each 105 cm long, or of two formed by the juxtaposition of shorter boards (35 and 55 cm). The shear strength of the glue line (f_{v0}), modulus of elasticity (E_{c90}), and strength (f_{c90}) in compression perpendicular to the grain; delamination (DL); and main and extended glue line thicknesses were evaluated. The Resistograph equipment was used to perform the perforation perpendicular to the glue line (samples extracted from the glulam elements) to correlate the properties. The results of this research demonstrate that the scheme of the boards had little effect on the physical and mechanical properties evaluated (except the main glue line and delamination), and the drilling resistance (DR) presents a significant correlation with practically all properties evaluated (variations in density values and other properties are explained by variations in DR values), making it possible to estimate E_{c90} and f_{c90} with desired precision ($R^2_{adj} \approx 80\%$). This highlights the feasibility of using this methodology in the quality control of glulam elements. It is concluded that regardless of the adhesive, elements comprising a 105 cm-length core and external lamellae (T1 and control) are indicated for external use, presenting low delamination. Short-length central lamellae adhesively glued with PUR (T2) are not recommended for external applications due to their susceptibility to delamination. However, T2 is indicated for internal environments due to its low production cost. This study also proved the efficiency of using models based on drilling resistance to estimate wood density and its resistance to compression perpendicular to the fiber.

Keywords: glue line; polyurethane; physical and mechanical properties; resorcinol; glulam; drilling resistance

Citation: Oliveira, R.F.; Segundinho, P.G.d.A.; da Silva, J.G.M.; Gonçalves, F.G.; Lopes, D.J.V.; Silva, J.P.M.; Lopes, N.F.; Mastela, L.d.C.; Paes, J.B.; de Souza, C.G.F.; et al. Eucalyptus-Based Glued Laminated Timber: Evaluation and Prediction of Its Properties by Non-Destructive Techniques. *Forests* **2024**, *15*, 1658. https://doi.org/10.3390/f15091658

Academic Editors: Anuj Kumar and Milan Gaff

Received: 8 June 2024
Revised: 8 August 2024
Accepted: 16 August 2024
Published: 20 September 2024

1. Introduction

Several Eucalyptus species have been studied as possible raw materials for structural elements of glulam [1–4]. Expanding the potential of commercially available hardwood species as a raw material for the manufacture of glulam, these Eucalyptus species are viable due to their mid-range density (450 to 750 kg·m^{-3}), bending strength, and modulus of elasticity (MOE), which are higher or comparable to those of commonly used softwoods, as well as their distinct colors and natural patterns [5–7]. However, because of their mid-range density, the structural elements of glulam from Eucalyptus species have the potential to promote effective bonds, creating a stronger light-moderate weight and distinctly colored product. Thus, stakeholders may be encouraged to successfully introduce these elements into the market as a direct consequence. The production of Eucalyptus-planted forests is a sustainable option in the face of deforestation of natural forest biomes. Planted forests are used economically as a source of wood; however, during their growth they provide important ecosystem services for the environment, such as carbon capture and storage, soil cover preventing erosion, and habitat for numerous species of animals [8,9].

To further market acceptance, the adhesive used to produce Eucalyptus glulam needs to be environmentally friendly, comply with governmental regulations, and promote sustainability. Over the last 18 years, the solvent-free castor bean byproduct has been extensively used in the production of particleboard, plywood, and glulam due to its bonding performance [10–13]. Thus, the solvent-free bicomponent castor oil-based polyurethane (PUR), comprising pre-polymer and polyol parts, agrees with the new market expectations and regulations as well as shows competitive wettability, swelling, and internal bonding strength [13,14].

Several authors [13,14] pointed out that PUR has higher wettability than resorcinol formaldehyde (RF) on Eucalyptus, indicating better adhesive penetration. Additionally, it exhibits lower thickness swelling rates and higher interbond strength compared to formaldehyde-based adhesives for wood composites. Furthermore, to ensure the potential utilization of the PUR application in Eucalyptus glulam, its performance should be comparable to commercially available adhesives as they have a track record of high performance. To this end, one of the authors' research objectives was to test the performance of the PUR adhesive and compare it to RF.

The adhesion performance is ensured by testing the glue line through available methods such as cleavage/tensile and shear strength, delamination, and wood failure estimate [15]. Adhesion performance testing should also include image evaluations of the glue line and thickness measurements, which allow inferences about the adhesive's penetration into the wood and the physical conditions of the glue line formed. These conditions, including starved, optimal, or thick glue lines, as well as the presence of holes, cracks, air bubbles, and other visible defects, are critically important [15–18]. Microscopy is commonly used to evaluate the durability of the adhesion line in laminated wood, observing that the anatomy of the wood, the type of adhesive, and the pressure imposed on the laminated boards directly influence the penetration of the adhesives [19].

Robust, trustworthy, and safe methods of evaluating structural elements should be conducted to further Eucalyptus glulam acceptance and utilization. To that end, the Resistograph drilling resistance (DR) is investigated in this research. This non-destructive technique is well established in the evaluation of the physical properties of wooden poles, standing trees, and structurally important wooden elements [20–25]. The use of DR can be enhanced by adjusting mathematical models that correlate wood density and moisture [26]. In this case, the use of DR could be evaluated by linear regression models to estimate the physical and mechanical properties of glulam elements.

The objective of this study was to understand the influence of assembly schemes (cores composed of continuous and discontinuous parts) of glulam elements in conjunction with the use of PUR and resorcinol formaldehyde adhesives. Additionally, the study aimed to evaluate the correlation between puncture resistance and other properties of laminated wood. Furthermore, based on the accuracy of the regression models, the study sought to

validate the use of the Resistograph as an auxiliary tool in controlling the production of Eucalyptus glulam elements.

2. Materials and Methods

2.1. Materials, Sampling, and Assembly of Glulam Elements

Eucalyptus (clone *Eucalyptus urophylla* × *Eucalyptus grandis*) boards were graded according to the American Standard for Testing and Material—ASTM D 245 [27] to compose 15 glulam elements (105 × 10.5 × 10) cm^3 (length × thickness × width), with 5 elements per experimental condition (Table 1). These boards were traded under the brand Lyptus® from 11-year-old trees, as they were available in the state of Espirito Santo, Brazil. Each glulam element was produced for gluing four lamellae by applying 300 $g \cdot m^{-2}$ of adhesive in a simple glue line for bonding [28]. The glulam elements were divided into one control (T3) and two treatments (T1 and T2), as described in Table 1. Each element comprised two core lamellae and two external lamellae. In T2, one of the two central lamellae is made up of three 35 cm-long boards, and the other of two 55 cm-long boards. The sample extraction layout in the T2 treatment avoided butt-joint regions.

The adhesives used were Resorcinol-formaldehyde (RF), known as Cascophen RS216M (Casco®, Hexion) in addition to 20% catalyst and bicomponent castor oil-based polyurethane (PUR) (Imperveg® AGT 1315) in a 1:1.2 ratio (prepolymer: polyol) [29]. These 15 elements were pressed for 48 h, at 1.0 MPa, in a hydraulic press (Bovenau, P15000) [29]. Later, they were flattened and sectioned to a final dimension (100 × 10 × 10) cm^3 (length × thickness × width), as shown in Figure 1, for different tests.

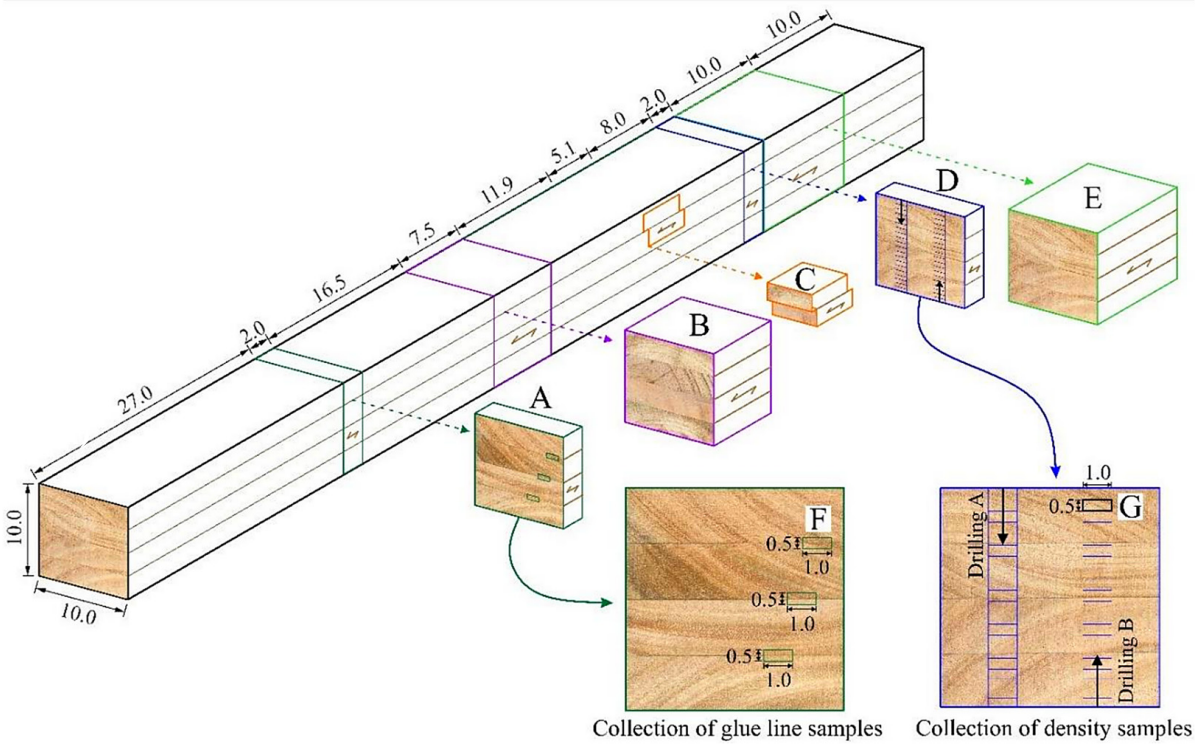

Figure 1. The sampling scheme of the glulam elements, with color emphasis for the samples (measured in centimeters) used in this study. (A): cross-sectional sample for glue line; (B): delamination sample; (C): shear strength samples; (D): Resistograph drilling resistance sample; (E): Compression perpendicular to grain sample; (F): glue line sample; (G): density sample of the perforated sections after obtaining the Resistograph drilling resistance.

Table 1. Composition and characteristics of the treatments.

Treatments	Description	Adhesive	Repetition
T1	Elements comprising 105 cm-length core and external lamellae	PUR (bicomponent castor oil-based polyurethane)	5
T2	Elements comprising short-length core lamellae (35 to 55 cm) bonded by end joints, and 105 cm-length external lamellae	PUR (bicomponent castor oil-based polyurethane)	5
Control (T3)	Elements comprising 105 cm-length core and external lamellae	RF (resorcinol-formaldehyde)	5

2.2. Delamination Test and Shear and Compressive Strength Test

Fifteen samples, each one with the dimensions (7.5 × 10 × 10) cm^3 (Figure 1—Sample B), were meticulously prepared for the delamination test on the glue line, adhering to the guidelines set forth by the American Institute of Timber Construction (AITC T110) [30].

The other fifteen samples (Figure 1—Sample C) were meticulously prepared for shear testing on the glue line, following the ASTM D 905 standard [31]. After shearing, the wood failure percentages were determined by analyzing transparent slide patterns by ASTM D 5266 [32].

Additionally, another set of fifteen samples, measuring (10 × 10 × 10) cm^3 (Figure 1—Sample E), were subjected to a mechanical test in a gantry system. The Catman® software (HBM, Catman Easy 5.2, Darmstadt, Germany) was utilized to collect data for evaluating the compressive strength perpendicular to the grain (f_{c90}) of the glulam. The loading procedure was adapted from ASTM D143 [33], with the loading curve processed until the samples exhibited 2.5 mm. The modulus of elasticity (E_{c90}) was obtained based on the ABNT NBR 7190-3 (2022) [34].

2.3. Glulam Main and Extended Glue Line Thickness

Histological slides with cross-sections of the glue line of the samples were used to measure the thickness of the main glue line (MGL) and extended glue lines (EGL) [16,17]. For this procedure, tree samples of uniform dimensions (2.5 × 1.0 × 0.5) cm^3 (Figure 1—F) were extracted from each glue line cross-section of the structural elements (Figure 1—A). These samples were boiled in distilled water for softening, and then histological sections of 20 µm were obtained using a sliding microtome. After this process, the histological slides were mounted using glycerin and distilled water solution.

For analysis, five images from each histological slide of the glue line were obtained using a 5 X objective lens in an optical microscope with a digital camera (Zeiss, Axio Scope A1, Oberkochen, Germany) (Figure 2). Following image acquisition, the main glue line (MGL) was defined as the glue line width. EGL was defined as the left and right extension from MGL up to the last lumen filled with adhesive. The measurements of the glue line thickness were performed using the Fiji platform, a distribution of the open-source software ImageJ in micrometers (µm) [35,36].

Finally, six glue line thicknesses of MGL and EGL were measured and evenly distributed in each image, totaling 30 measurements of MGL and EGL per glue line and 450 measurements of MGL and EGL per treatment (6 measured lengths × 5 images × 5 structural elements = 450 measurements of MGL and EGL per treatment), as illustrated in Figure 2.

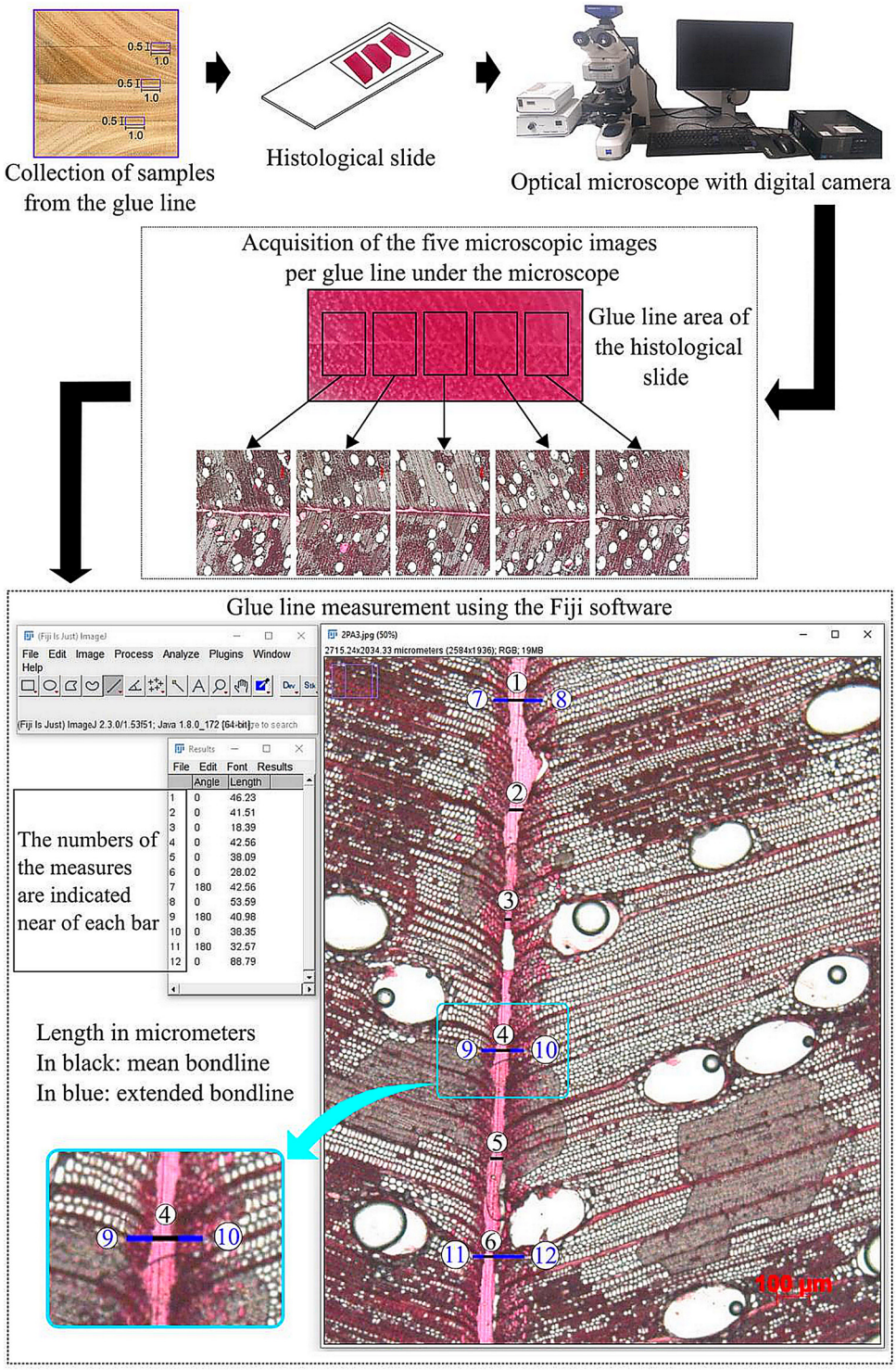

Figure 2. Main and extended glue line thickness acquisition through microscopic images of glue line samples.

2.4. Resistograph Drilling Resistance and Wood Densities

Fifteen cross-sectional samples, each measuring (2.5 × 10 × 10) cm^3 and corresponding to a single glulam element (Figure 1—D), were meticulously prepared for the assessment of Resistograph drilling resistance (DR) and the determination of densities. Initially, these samples underwent air-seasoning until a constant mass was achieved (temperature 25 °C, relative humidity of air 65%, and moisture content of samples 12%). Following stabilization, each sample was drilled twice in opposite directions to obtain an averaged DR value,

utilizing the Resistograph (RINNTECH, R650-SC, Heidelberg, Germany) as shown in Figure 3. The feeding rate for drilling was maintained at 20 mm s^{-1}.

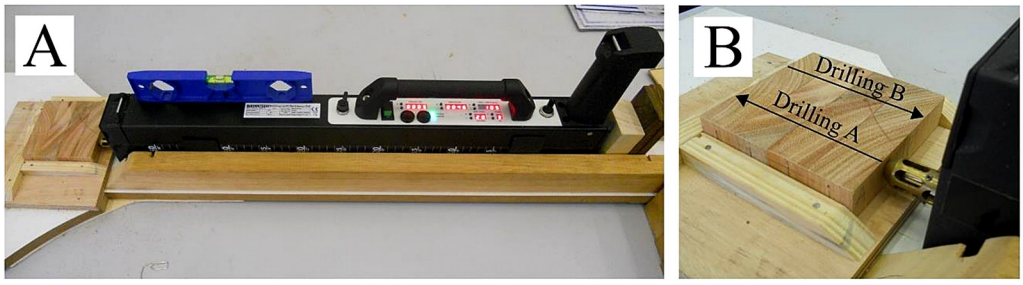

Figure 3. Drilling with Resistograph to obtain drilling resistance. Arrow refers to the direction of drilling the rod of the equipment along the three lines of glue of the test sample. (**A**) Leveling of drilling equipment; (**B**) Positioning the sample during drilling.

For the determination of basic density (BD), density at 12% moisture content ($D_{12\%}$), and density at 0% moisture content ($D_{0\%}$) of the wood, samples were collected at 0.5 cm intervals from the locations corresponding to the perforations made with the Resistograph (Figure 1—F). The calculations for BD, $D_{12\%}$, and $D_{0\%}$ were performed according to the ABNT NBR 7190-2 (2022) [37].

The Resistograph records the DR data in its internal memory. The data points refer to the electronic energy consumption of the rotating motor ranging from 0 to 4095 rpm, as the drilling of the steel rod with constant feed speed begins [38,39]. To this end, the data were standardized, simplified, and represented as a percentage. This data processing step agrees with the previous literature [23,24].

2.5. Data Analysis

The experiment was installed under a completely randomized design (CRD). An analysis of variance (ANOVA) was performed to evaluate the effects of the treatments (T1, T2, and T3—see Table 1). When significant differences were identified for BD, $D_{12\%}$, $D_{0\%}$, perpendicular compressive strength (f_{c90}), modulus of elasticity to perpendicular compression (E_{c90}), shear strength in the glue line (f_{v0}), wood failure percentage (WF), delamination (DL), extended glue line (EGL), and main glue line (MGL) by the F-Test ($p < 0.05$), the post hoc Tukey test ($p < 0.05$) was used. The assumptions of ANOVA of residual normality and homogeneity of variances were evaluated by the Shapiro–Wilk ($p < 0.05$) and Bartlett ($p < 0.05$) tests, respectively.

Pearson's correlation ($p < 0.05$) was used to verify the functional relationships between the DR and the variables BD, $D_{0\%}$, $D_{12\%}$, f_{c90}, E_{c90}, f_{v0}, DL, EGL, and MGL. For the variables considered as significant in Pearson's correlation, linear regression models were adjusted. Only the most relevant linear models were presented (BD, $D_{0\%}$, $D_{12\%}$, f_{c90}, and E_{c90}). The regression models were analyzed by the significance of all coefficients of the equation (t-test, $p < 0.05$). Linear regression models' predictive performance was analyzed by the adjusted coefficient of determination (R^2_{aj}) and root means square error (RMSE). The leave-one-out cross-validation was performed using the R programming language, version 4.3.2 [40] under a software environment to verify the generalization capability of the adjusted models. Residual dispersion plots were generated for the adjusted and validation data to complement the regression analysis.

3. Results and Discussion

3.1. Physical-Mechanical Properties of Glulam Elements

Statistical differences were only found for the main glue line (MGL) and delamination (DL) (Table 2). The glulam glued with bicomponent castor oil-based polyurethane (PUR) presented similar strength for resorcinol-formaldehyde (RF—control or T3 treatment; Table 1). This result demonstrates the real potential of PUR as an adhesive to produce

both Eucalyptus glulam treatments (T1 and T2; Table 1). Consequently, this approach not only ensures sustainability but also contributes to cost reduction in glulam production by utilizing shorter boards in the core lamellae.

Table 2. Mechanical and physical properties of Eucalyptus glulam by treatments.

Properties		Treatments		
		T1	T2	Control
Shear 12%	f_{v0} (MPa)	9.06 a (1.78)	10.08 a (1.16)	9.86 a (1.84)
	WF (%)	81.00 a (29.38)	94.00 a (7.41)	96.50 a (2.09)
Compression perpendicular to the grain 12%	f_{c90} (MPa)	6.77 a (2.23)	6.58 a (1.14)	5.51 a (1.19)
	E_{c90} (MPa)	513.97 a (186.81)	457.47 a (81.19)	390.80 a (113.62)
Basic density (BD) (g·cm^{-3})		0.46 a (0.08)	0.49 a (0.05)	0.43 a (0.04)
Density at 12% ($D_{12\%}$) (g·cm^{-3})		0.56 a (0.11)	0.60 a (0.07)	0.56 a (0.09)
Density at 0% ($D_{0\%}$) (g·cm^{-3})		0.53 a (0.10)	0.57 a (0.07)	0.51 a (0.06)
Main glue line (MGL) (µm)		33.26 b (14.71)	39.35 b (13.57)	79.80 a (17.44)
Extended glue line (EGL) (µm)		55.83 a (21.60)	64.67 a (15.49)	40.43 a (11.17)
Delamination (DL) (%)		7.92 ab (14.09)	27.42 a (23.32)	0.29 b (0.66)
Drilling resistance (DR) (%)		90.68 a (31.86)	83.80 a (18.37)	74.01 a (14.18)

Means followed by the same letter on the line do not differ (Tukey, $p > 0.05$). The standard deviation is shown in parentheses.

The shear strength (f_{v0}), wood failure percentage (WF), compression strength perpendicular to the grain (f_{c90}), and modulus of elasticity (E_{c90}) in compression perpendicular ranged within the limits (Eucalyptus glulam) found in the literature (Table 3). It is hypothesized that the variation among the obtained values may occur due to the age and species of Eucalyptus, the proportion of adhesives, and the bonding processes employed.

In addition, specific reactions of wood and the type of adhesive during bonding might contribute to the observed variations. However, it is essential to consider the differences between species, ages, and edaphoclimatic conditions of the growth sites, because they influence several growth and physical parameters. The formation of earlywood and latewood, characterized by mature wood in older trees composed of fibers with a consolidated wall structure, positively influences mechanical resistance. Additionally, variations in the proportions of heartwood and sapwood affect the functionality of sap conduction in parts of the wood, as well as its permeability, natural durability, and consequently, variations in density and grain angle radially and longitudinally to the stem [38,39,41], as observed, for example, in the high variability of the data for compression perpendicular to the grain 12%.

Table 3. Results in the literature of mechanical and physical properties of Eucalyptus glulam.

Species (Years)	Ad	Basic Density ($g \cdot cm^{-3}$)	Spread Rate ($g \cdot m^{-2}$)	f_{v0} (MPa)	WF (%)	f_{c90} (MPa)	E_{c90} (MPa)	De (%)	MGL (µm)	EGL (µm)	Reference
Eucalyptus grandis × *urophylla* (11y)	PUR	<0.58	250	7.26	N/A	6.70	N/A	0.00	3.17	51.77	[17,29]
	RF	<0.58	250	7.84	N/A	6.39	N/A	0.00	125.22	278.18	
Eucalyptus spp. (7–10y)	PUR	0.51	300	12.68	79.58	10.61	493.0	N/A	24.25	N/A	[42]
	RF	0.54	300	10.40	93.50	8.68	476.75	N/A	80.31	N/A	
Eucalyptus spp.	PUR	0.67	250	8.10	71.10	N/A	N/A	N/A	100.70	N/A	[14,18]
	RF	0.67	250	6.73	29.75	N/A	N/A	N/A	41.80	N/A	
Eucalyptus cloeziana (6–8y)	PUR	0.62	150	8.29	44.16	N/A	N/A	14.91	13.41	15.79	[3]
	RF	0.62	150	11.44	91.88	N/A	N/A	0.00	52.13	60.23	
Eucalyptus spp.	RF	N/A	N/A	7.75	N/A	N/A	N/A	13	N/A	N/A	[2]
Eucalyptus spp.	RF	N/A	300–350	3.80	N/A	N/A	N/A	38	N/A	N/A	[1]
Eucalyptus grandis (18y)	RF	0.55	250	4.72	93.04	N/A	N/A	N/A	129.0	N/A	[16]

Ad: adhesive; f_{v0}: shear strength; WF: wood failure percentage; f_{c90}: compression strength perpendicular to the grain; E_{c90}: modulus of elasticity to compression perpendicular; De: delamination; MGL: main glue line; EGL: extended glue line; PUR: bicomponent castor oil-based polyurethane; RF: resorcinol-formaldehyde and N/A: not available.

The samples glued with RF (T3) resulted in a higher main glue line (MGL) mean than those glued with PUR (T1 and T2), while the mean of the extended glue line (EGL) for T1 and T2 was higher (Table 2 and Figure 4). The highlighted area in Figure 5 illustrates the differences in EGL between PUR and RF, emphasizing the number of filled cells' lumens in each treatment. It is worth noting that fewer filled cells' lumens exist in T3. Also, some gas bubbles are present in the PUR and RF glue lines, creating a discontinuous space in the MGL. This characteristic was observed in several images of glue lines. The spaces formed in the MGL can negatively affect the bonding capacity of the adhesive with the wooden pieces, resulting in low durability. Empty spaces with the presence of bubbles were also observed in studies with the species *Eucalyptus tetodonta* when using PUR and RF adhesives [43]. Regarding PUR adhesive, some authors claim that it reacts chemically with water, inducing the release of carbon dioxide, thus explaining the presence of bubbles. Other factors involved are related to the preparation of the adhesive and application to the glue line, as well as the shrinkage of the adhesive [44].

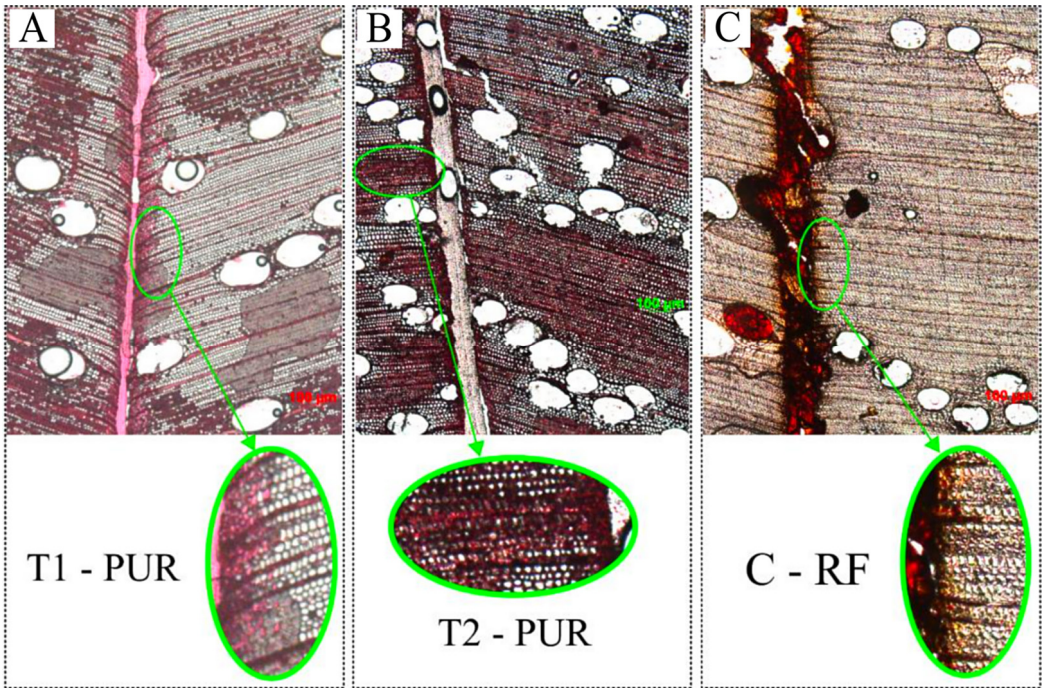

Figure 4. Microscope images of glue line samples. The highlighted area focuses on the filled cells' lumens with adhesive. (**A**) T1 (treatment 1), (**B**) T2 (treatment 2), and (**C**) T3 (control): see Table 1; PUR: bicomponent castor oil-based polyurethane; RF: and resorcinol-formaldehyde drilling with Resistograph to obtain drilling resistance.

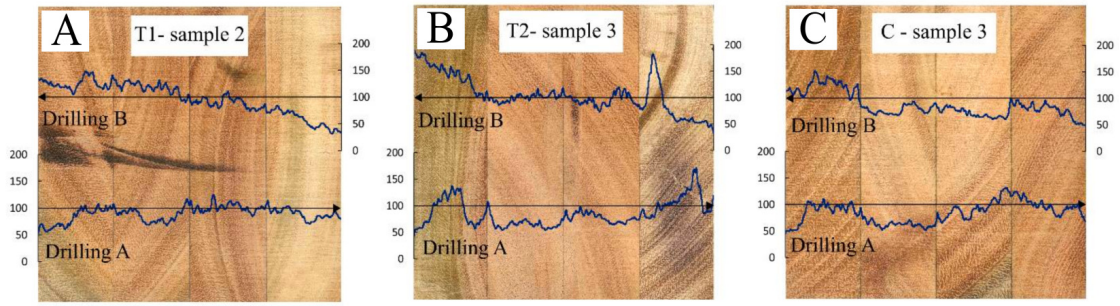

Figure 5. Examples of drilling resistance profiles (percentage values) in the cross-sections of Eucalyptus glulam elements. (**A**) T1, (**B**) T2, and (**C**) T3: see Table 1. The black arrow indicates the direction of penetration of the Resistograph rod.

The characteristics of the PUR adhesive, such as effective wetting of substrate surfaces, formation of polar bonds, relatively low molar mass, and small molecular size allowing penetration into the pores of substrates, might have been responsible for their greater penetration into the wood and, consequently, the higher EGL and lower MGL [45].

Not only does increased adhesive penetration into the wood confer greater resistance and stability of the bond, but the form of penetration and the chemical composition of the surface should also be considered to ensure adhesion and resistance [2,46]. Therefore, it is essential to observe, in the histological sections of the glue lines, whether the adhesive created interval penetrations (non-uniform penetration), an adjacent adhesive section (shallow and uniform penetration in a section adjacent to the main glue line), or an interpenetrating polymerization network (uniform penetration with sufficient depth to configure a consistent locking section) [47]. By gathering resistance and glue line thickness information (Table 2) and the glue line penetration formats (Figure 4), we concluded that T2 showed interval penetrations and T1 and T3 exhibited adjacent adhesive sections.

Both T1 (PUR) and T3 (RF), with less than 8% delamination, are suitable for external use according to AITC T110 [30] and have values below those reported in the literature (see Table 3). However, T2 delamination (PUR) values did not meet the limit recommended by the standard. The short-length core lamellae bonded by end joints affected the delamination percentage in Eucalyptus glulam glued with PUR. The volumetric shrinking and swelling of the short-length core lamellae created tensions on the glue line higher than the PUR adhesive was able to support.

Although the means of Resistograph drilling resistance (DR) did not differ statistically among treatments, higher absolute values are observed for treatments glued with PUR (T1 and T2) (Table 2). This may be explained by the internal variation of the woods used in these treatments, which had some growth rings with thicker-walled cells, increasing the DR values. This behavior can be visualized in the regions with the highest peaks in the DR measurements, specifically corresponding to the latewood (darker colors) of the growth rings (Figure 6). For instance, the mean values of basic density for sample 2 of T1, sample 3 of T2, and sample 3 of T3 are 0.56, 0.60, and 0.53 g·cm^{-3}, with mean DR values of 93.0%, 93.5%, and 84.7%, respectively.

Each lamella exhibits different drilling resistance (DR) profiles depending on the specific region where the drilling was performed (Figure 5), potentially impacting the DR readings. However, the adoption of two opposite drilling directions enabled the recording of distinct DR values in the same lamella. This approach facilitated the calculation of a representative mean, allowing for a more comprehensive sampling of the element.

The DR measurements, taken as averages every 0.5 cm, aligned with the density profiles obtained at the drilling sites as shown in Figure 6. Averages from two perforations in opposite directions were utilized to compose the profile of a section of the glulam element. Consequently, the drilling resistance provided a satisfactory record of the density profiles and the physical structure of the glulam elements. This method holds potential for evaluation in the quality control of produced beams and inspections of elements in service, as demonstrated in the case of treated wooden poles [24], glulam [20], and wood bridges [25].

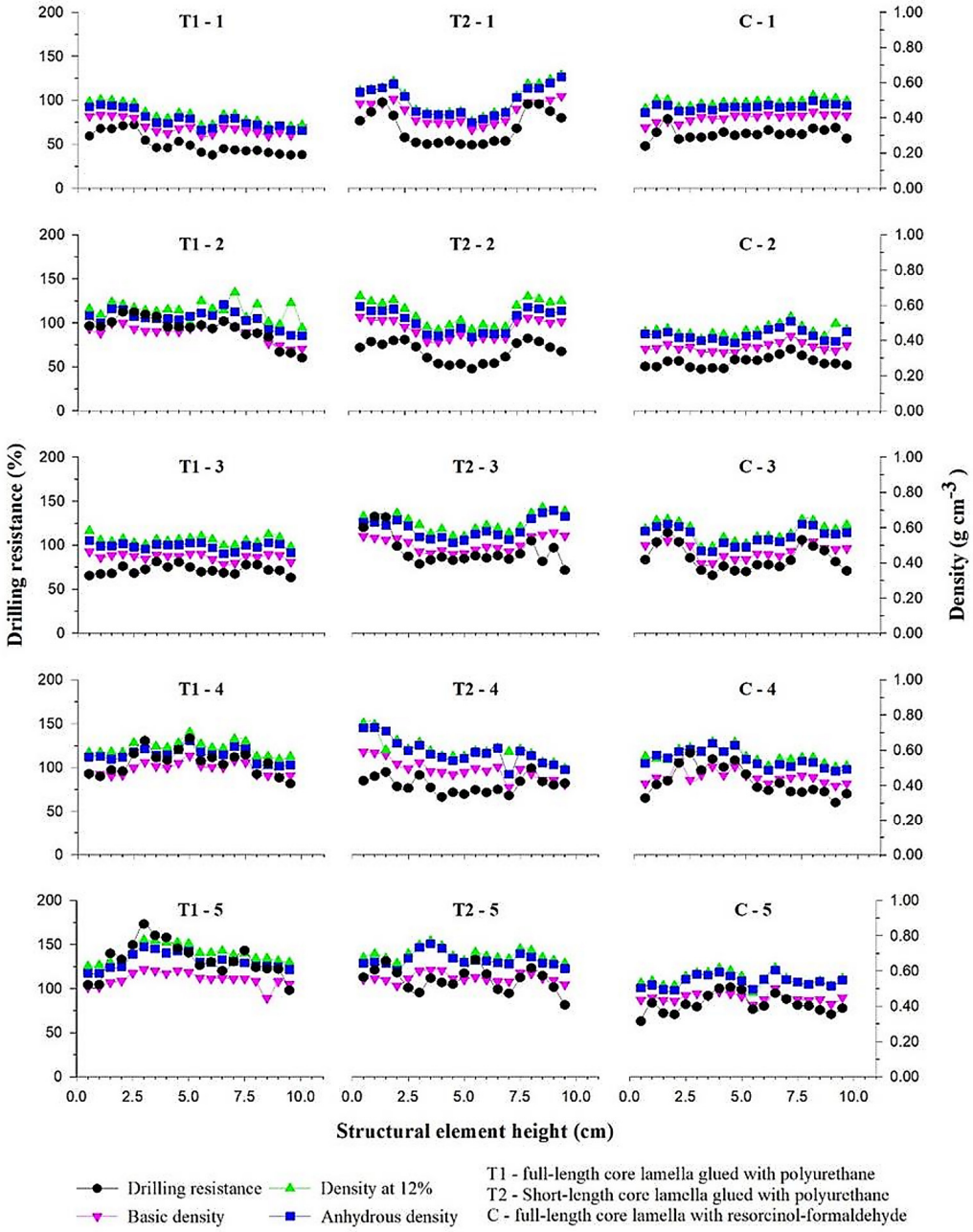

Figure 6. Profiles of drilling resistance (DR) averages and densities along the cross-sections for all glulam elements, with measurements obtained every 0.5 cm.

3.2. Estimative of the Physical-Mechanical Properties of Glulam by Drilling Resistance

The Pearson's correlation matrix of the physical-mechanical properties of the glulam elements was calculated using the 15 samples. The matrix revealed the absence of significant correlations between MGL and the other properties (Figure 7). Furthermore, the correlation analysis also showed no significant correlations between DL and f_{c90}, E_{c90}, and f_{v0}, as well as between f_{v0} and EGL.

The degrees of correlation of DR are strong and positive with BD, $D_{0\%}$, $D_{12\%}$, f_{c90}, and E_{c90}, and average and positive with DL, EGL, and f_{v0}. The correlation between DR and densities of the glulam elements is at the superior limit of the generally observed amplitude of this variable (r) for Eucalyptus species [26].

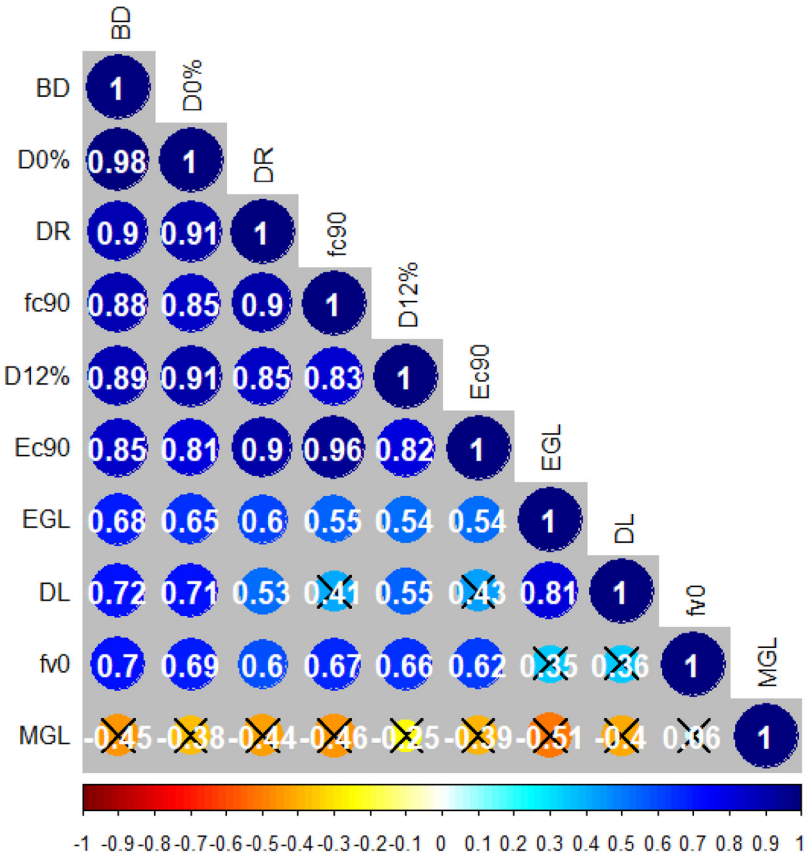

Figure 7. Pearson correlation matrix of the physical-mechanical properties of Eucalyptus glulam elements. Values within the circle are the correlation coefficients (r). Circles marked with X are not significant (*t*-test, $p > 0.05$). BD: basic density; $D_{0\%}$: density at 0% moisture content; DR: drilling resistance; f_{c90}: compression strength perpendicular to the grain; $D_{12\%}$: density at 12% moisture content; E_{c90}: Modulus of elasticity to compression perpendicular; EGL: extended glue line; DL: delamination; f_{v0}: shear resistance in the glue line; MGL: main glue line.

The positive correlation between DL and EGL, and the negative but not significant correlation between DL and MGL, indicate that the highest EGL was not able to resist delamination due to the influence of T1 and T2 with higher EGL. Higher MGL, however, demonstrated resistance against delamination, as observed in T3. Considering the characteristics of each adhesive, in this study, the highest MGL was shown to be more effective against delamination.

EGL positively correlates with BD, $D_{0\%}$, and $D_{12\%}$, indicating a higher penetration of adhesives with an increase in density that should indicate an increment in f_{v0}. However, this was not observed (Table 2). This effect occurred mainly because of the PUR adhesive in T1 and T2, which penetrated more into the wood, even in denser lamellae. Figure 6 shows that the densities of the glulam elements of T3 did not exceed 0.60 g·cm^{-3}, while the samples of T1 and T2 exceeded certain lamellae.

Based on the profiles presented (Figures 6 and 7) and correlation values (Figure 8), it is possible to affirm that drilling resistance (DR) showed a functional relationship with all properties, except MGL. Thereby, DR could estimate these variables and record the internal variations of wood that occurred in the lamellae of glulam. In this case, eight regression models were adjusted, with DR as an independent variable, except for MGL, where the correlation with DR was not significant. Among these eight models, five were considered most relevant, with R^2_{aj} greater than 0.69, with a variation from 0.7 to 0.81 as shown in Table 4.

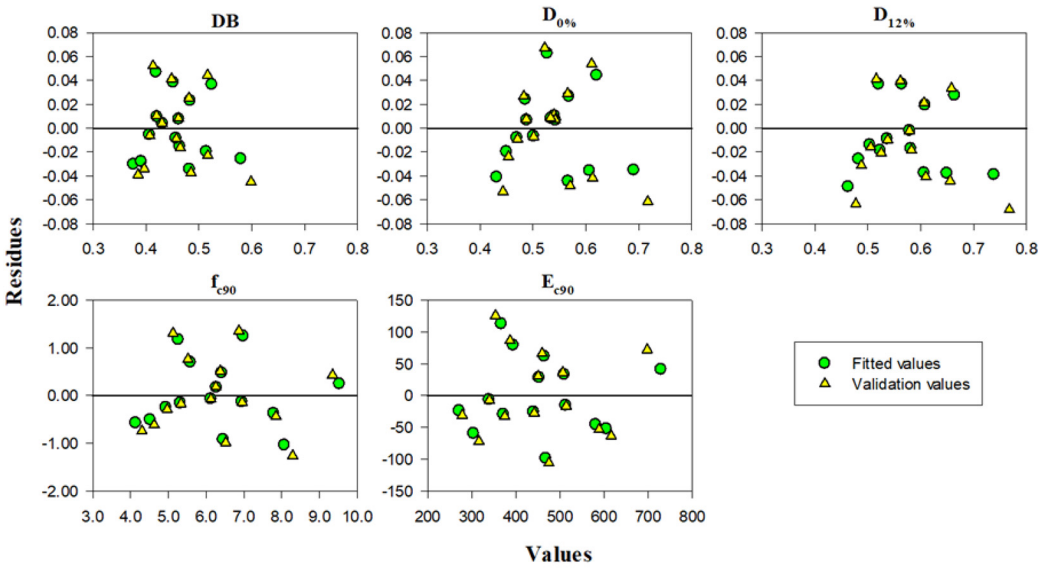

Figure 8. Dispersion of the residues of the adjustment and validation of the models of the physical-mechanical properties of Eucalyptus glulam. BD: basic density; $D_{0\%}$: density at 0% moisture content; $D_{12\%}$: density at 12% moisture content; f_{c90}: compression strength perpendicular to the grain; E_{c90}: modulus of elasticity to compression perpendicular.

Table 4. Mathematical models adjusted and validated to estimate physical-mechanical properties of glulam elements as a function of drilling resistance.

Models	R^2_{aj}	RMSE	R^2_{CV}	$RMSE_{CV}$
BD = 0.255354 * + 0.002437 × DR	0.79	0.0258	0.73	0.0308
$D_{12\%}$ = 0.298655 * + 0.03308 × DR	0.70	0.0437	0.64	0.0503
$D_{0\%}$ = 0.276592 * + 0.003116 × DR	0.81	0.0306	0.75	0.0371
f_{c90} = 0.92310 ^{ns} + 0.06472 × DR	0.80	0.6572	0.76	0.7491
E_{c90} = 0.89810 ^{ns} + 5.4930 × DR	0.80	55.9220	0.76	64.0361

R^2_{aj}: adjusted coefficient of determination; RMSE: root mean square error; R^2CV: coefficient of determination of cross-validation; RMSECV: root mean square error cross-validation; ns: not significant (*t*-test, $p > 0.05$); *: significant (*t*-test, $p < 0.05$); BD: basic density; DR: drilling resistance; $D_{0\%}$: density at 0% moisture content; $D_{12\%}$: density at 12% moisture content; f_{c90}: compression strength perpendicular to the grain; and E_{c90}: modulus of elasticity to compression perpendicular to the grain.

Apart from densities, only f_{c90} and E_{c90} achieved an adjusted $R^2_{aj} > 0.79$ with DR, and these properties exhibited Pearson's correlations of 0.90 with DR and above 0.81 with densities (Figure 8). This result is likely attributed to the direct relationship between compression strength perpendicular to the grain and material density. Therefore, a connection with density implies a predisposition for the existence of a relationship with DR. On the other hand, DL, EGL, and f_{v0} were positively correlated with DR (r = 0.53 and 0.60). However, the R^2_{aj} for adjusted models was lower (<0.50). The low R^2_{aj} of the DL, EGL, and f_{v0} models were due to their weaker relationship with the density of the material.

Among the five better models, the largest difference observed between R^2_{aj} and R^2CV was 9% (0.06), as seen in the $D_{12\%}$ model. From the residue dispersion plots (Figure 8), it is evident that the adjusted models were randomly dispersed. This statistical observation indicates that the regression models were generalizing properly, and there is potential for them to generalize well with truly unseen data.

4. Conclusions

Based on the results obtained from this research, it is concluded that:

- Treatments T1 and control, consisting of full-length core lamellae, demonstrate effectiveness for external use due to lower delamination (less than 8%) and positive evaluations of their physical and mechanical properties;
- Treatment T2, comprising short-length core lamellae, is not recommended for external use due to delamination exceeding 8%. However, T2 shows promise for internal use because of its potential to reduce production costs using short-length core lamellae and a sustainable adhesive;
- Drilling resistance proves to be a valuable tool for recording functional relationships between physical and mechanical properties in the wood across each lamella of the glulam elements, except MGL;
- Linear regression models based on drilling resistance made it possible to estimate, with desired accuracy ($R^2_{adj} \approx 80\%$), the wood density as well as strength and stiffness in compression perpendicular to the grain;
- The results can be considered indicative; however, an increase in the number of specimens in future research is suggested, and it is expected that the conclusions will corroborate the current ones.

Author Contributions: R.F.O.: Methodology, Formal Analysis, Data Curation, Investigation, and Writing—Original Draft Preparation. P.G.d.A.S.: Conceptualization, Writing—Review and Editing, Funding Acquisition, and Supervision. F.G.G., D.J.V.L., and F.A.R.L.: Writing—Review and Editing. J.B.P., and A.L.C.: Formal Analysis, Writing—Review and Editing. L.d.C.M., J.G.M.d.S., J.P.M.S., N.F.L., C.G.F.d.S., M.A.R.B., and C.P.d.A.: Data Curation and Writing—Original Draft Preparation. All authors have read and agreed to the published version of the manuscript.

Funding: This research was funded by the Espírito Santo State Foundation for the Support of Research and Innovation (FAPES/SEAG notice No. 06/2015—PPE AGROPECUÁRIA) grant number (T.O. No. 720/2016). And The APC was funded by the Espírito Santo State Foundation for the Support of Research and Innovation (FAPES notice No. 18/2023—Publication of technical-scientific articles—Cycle 4).

Data Availability Statement: Data is contained within the article.

Acknowledgments: The Espírito Santo State Foundation for the Support of Research and Innovation (FAPES) for the financial support and the Federal University of Espirito Santo (UFES).

Conflicts of Interest: The authors declare no conflicts of interest and had no role in the design of the study; in the collection, analysis, or interpretation of data; in the writing of the manuscript; or in the decision to publish the results.

References

1. Calil Neto, C.; Christoforo, A.L.; Ribeiro Filho, S.L.M.; Lahr, F.A.R.; Calil Junior, C. Avaliação da resistência ao cisalhamento e à delaminação em madeira laminada colada. *Ciência Florest* **2014**, *24*, 989–996. [CrossRef]
2. de Almeida, D.H.; Cavalheiro, R.S.; de Macêdo, L.B.; Neto, C.C.; Christoforo, A.L.; Junior, C.C.; Lahr, F.A.R. Evaluation of quality in the adhesion of glued laminated timber (Glulam) of paricá and lyptus wood species. *Int. J. Mater. Eng.* **2014**, *4*, 114–118. [CrossRef]
3. Segundinho, P.G.A.; Gonçalves, F.G.; Gava, G.C.; Tinti, V.P.; Alves, S.D.; Regazzi, A.J. Eficiência da colagem de madeira tratada de *Eucalyptus cloeziana* F. Muell para produção de madeira laminada colada (MLC). *Rev. Mater.* **2017**, *22*, e11808. [CrossRef]
4. Chiniforush, A.A.; Akbarnezhad, A.; Valipour, H.; Malekmohammadi, S. Moisture and temperature induced swelling/shrinkage of softwood and hardwood glulam and LVL: An experimental study. *Constr. Build. Mater.* **2019**, *207*, 70–83. [CrossRef]
5. Aicher, S.; Ahmad, Z.; Hirsch, M. Bondline shear strength and wood failure of European and tropical hardwood glulams. *Eur. J. Wood Wood Prod.* **2018**, *76*, 1205–1222. [CrossRef]
6. Kovryga, A.; Stapel, P.; van de Kuilen, J.W.G. Mechanical properties and their interrelationships for medium-density European hardwoods, focusing on ash and beech. *Wood Mater. Sci. Eng.* **2020**, *15*, 289–302. [CrossRef]
7. Morin-Bernard, A.; Blanchet, P.; Dagenais, C.; Achim, A. Use of northern hardwoods in glued-laminated timber: A study of bondline shear strength and resistance to moisture. *Eur. J. Wood Wood Prod.* **2020**, *78*, 891–903. [CrossRef]
8. Brockerhoff, E.G.; Jactel, H.; Parrotta, J.A.; Quine, C.P.; Sayer, J. Plantation forests and biodiversity: Oxymoron or opportunity? *Biodivers. Conserv.* **2008**, *17*, 925–951. [CrossRef]
9. Sapucci, G.R.; Negri, R.G.; Massi, K.G.; Alcântara, E.H.D. Eucalyptus plantation benefits to patch size and shape of forested areas in Southeast Atlantic Forest. *Rev. Árvore* **2022**, *46*, e4626. [CrossRef]

10. Dias, F.M.; Lahr, F.A.R. Alternative castor oil-based polyurethane adhesive used in the production of plywood. *Mater. Res.* **2004**, *7*, 413–420. [CrossRef]
11. Azambuja, M.D.A.; Dias, A.A. Use of castor oil-based polyurethane adhesive in the production of glued laminated timber beams. *Mater. Res.* **2006**, *9*, 287–291. [CrossRef]
12. Silva, S.A.M.; Christoforo, A.L.; Ribeiro Filho, S.L.M.; Varanda, L.D.; Lahr, F.A.R. Particleboard manufactured with bicomponent polyurethane resin base on castor oil. *Int. J. Compos. Mater.* **2013**, *2*, 115–118. [CrossRef]
13. Chen, Y.-H.; Wu, C.-H.; Chen, Y.-C. Optimized condition for eco-friendly wood composites manufactured from castor oil-based polyurethane. *Constr. Build. Mater.* **2021**, *306*, 124789. [CrossRef]
14. Bianche, J.J.; Teixeira, A.P.M.; Ladeira, J.P.S.; Carneiro, A.d.C.O.; Castro, R.V.O.; Della Lucia, R.M. Cisalhamento na linha de cola de *Eucalyptus* sp. colado com diferentes adesivos e diferentes gramaturas. *Floresta E Ambient.* **2017**, *24*, 1–9. [CrossRef]
15. Frihart, C.R.; Hunt, C.G. Wood Adhesives: Bond Formation and Performance. In *Wood Handbook: Wood as an Engineering Material*; U.S. Department of Agriculture, Forest Service, Forest Products Laboratory: Madison, WI, USA, 2021; pp. 10.1–10.23.
16. do Sacramento Albino, V.C.; Mori, F.A.; Mendes, L.M. Estudo da interface madeira-adesivo de juntas coladas com resorcinol-formaldeído e madeira de *Eucalyptus grandis* w. Hill ex Maiden. *Sci. For.* **2010**, *38*, 509–516.
17. de Oliveira, R.G.E.; Gonçalves, F.G.; Segundinho, P.G.d.A.; Oliveira, J.T.d.S.; Paes, J.B.; Chaves, I.L.S.; Brito, A.S. Analysis of glue line and correlations between density and anatomical characteristics of *Eucalyptus grandis* × *Eucalyptus urophylla* glulam. *Maderas. Cienc. Y Tecnol.* **2020**, *22*, 495–504. [CrossRef]
18. Bianche, J.J.; Carneiro, A.d.C.O.; Vital, B.R.; de Andrade, B.G.; Gomes, R.M.; Araújo, S.d.O.; de Souza, E.C. Improving the understanding of wood bonding: Behavior of different adhesives on the surface of eucalyptus and pine wood. *Int. J. Adhes. Adhes.* **2022**, *112*, 102987. [CrossRef]
19. Masoumi, A.; Satir, E.; Adhikari, S.; Hindman, D.; Bond, B.; Zink-Sharp, A. Comparison of microscopy and quality control testing to examine the durability of adhesive bondline in cross-laminated timber. *J. Build. Eng.* **2024**, *86*, 108958. [CrossRef]
20. Teder, M.; Wang, X. Nondestructive evaluation of a 75-year-old glulam. In Proceedings of the 18th International Nondestructive Testing and Evaluation of Wood Symposium, Madison, WI, USA, 24–27 September 2013; Ross, R.J., Wang, X., Eds.; Department of Agriculture, Forest Service, Forest Products Laboratory: Madison, WI, USA, 2013; p. 8.
21. Rinn, F. Intact-decay transitions in profiles of density-calibratable resistance drilling devices using long thin needles. *Arboric. J.* **2016**, *38*, 204–217. [CrossRef]
22. Nowak, T.P.; Jasieńko, J.; Hamrol-Bielecka, K. In situ assessment of structural timber using the resistance drilling method-Evaluation of usefulness. *Constr. Build. Mater.* **2016**, *102*, 403–415. [CrossRef]
23. Oliveira, J.T.d.S.; Wang, X.; Vidaurre, G.B. Assessing specific gravity of young Eucalyptus plantation trees using a resistance drilling technique. *Holzforschung* **2017**, *71*, 137–145. [CrossRef]
24. Sharapov, E.; Brischke, C.; Militz, H. Assessment of preservative-treated wooden poles using drilling-resistance measurements. *Forests* **2019**, *11*, 20. [CrossRef]
25. Santos, D.A.S.; Gonçalves, F.G.; Segundinho, P.G.A.; Almeida, A.T.S.; Brito, L.D.; Chaves, I.L.S. Evaluation of pathological manifestations by non-destructive analysis techniques (NDT) in rural bridges. *Contrib. Cienc. Soc.* **2023**, *16*, 22108–22130.
26. Silva, J.G.M. Aplicação da Resistografia na Estimativa da Densidade e Umidade da Madeira em Árvores Jovens de Eucalipto. Ph.D. Thesis, Universidade Federal do Espírito Santo, Vitória, Brazil, 2019.
27. *ASTM D-245*; Standard Practice for Establishing Structural Grades and Related Allowable Properties for Visually Graded Lumber. ASTM (American Society for Testing and Materials): West Conshohocken, PA, USA, 2019; p. 17.
28. Plaster, O.B.; Oliveira, J.T.D.S.; Gonçalves, F.G.; Motta, J.P. Comportamento de adesão da madeira de um híbrido clonal de *Eucalyptus urophylla*× *Eucalyptus grandis* proveniente de três condições de manejo. *Ciência Florest.* **2012**, *22*, 323–330. [CrossRef]
29. Segundinho, P.G.A.; Oliveira, R.G.E.; Gonçalves, F.G.; Lopes, N.F.; Alves, R.C.; Azevedo, M.S. Evaluation of wood from the hybrid *Eucalyptus grandis* × *Eucalyptus urophylla* to be used in glued laminated timber. *Matéria* **2021**, *26*, e13030. [CrossRef]
30. *T110*; Test Methods for Structural Glued Laminated Timber-Cyclic Delamination Test. AITC (American Institute of Timber Construction): Centennial, CO, USA, 2007; p. 3.
31. *D-905*; Standard Test Method for Strength Properties of Adhesive Bonds in Shear by Compression Loading. ASTM (American Society for Testing and Materials): West Conshohocken, PA, USA, 2021; p. 5.
32. *D-5266*; Standard Practice for Estimating the Percentage of Wood Failure in Adhesive Bonded Joints. ASTM (American Society for Testing and Materials): West Conshohocken, PA, USA, 2020; p. 5.
33. *D-143-22*; Standard Test Methods for Small Clear Specimens of Timber. ASTM (American Society for Testing and Materials): West Conshohocken, PA, USA, 2022; p. 32.
34. *NBR 7190-3*; Parte 3: Métodos de Ensaio Para Corpos de Prova Isentos de Defeitos Para Madeiras de Florestas Nativas. ABNT (Associação Brasileira de Normas Técnicas).: Projeto de estruturas de madeira: Rio de Janeiro, Brazil, 2022.
35. Rasband, W.S. (1997–2015) ImageJ. National Institutes of Health, Bethesda, Maryland, USA. 2018. Available online: https://imagej.net/ij/ (accessed on 24 August 2024).
36. Schindelin, J.; Arganda-Carreras, I.; Frise, E.; Kaynig, V.; Longair, M.; Pietzsch, T.; Preibisch, S.; Rueden, C.; Saalfeld, S.; Schmid, B.; et al. Fiji: An open-source platform for biological-image analysis. *Nat. Methods* **2012**, *9*, 676–682. [CrossRef] [PubMed]
37. *NBR 7190-2*; Métodos de Ensaio Para Classificação Visual e Mecânica de Peças Estruturais de Madeira. ABNT (Associação Brasileira de Novas Técnicas): Rio de Janeiro, Brazil, 2022; p. 15.

38. Kloppenburg, A.M. Density determination of tropical hardwoods with the Resistograph. Master's Thesis, Delft University of Technology, Delft, The Netherlands, 2018.
39. Barbosa, T.L.; Oliveira, J.T.d.S.; Rocha, S.M.G.; Câmara, A.P.; Vidaurre, G.B.; Rosado, A.M.; Leite, F.P. Influence of site in the wood quality of Eucalyptus in plantations in Brazil. *South. A J. Sci.* **2019**, *81*, 247–253. [CrossRef]
40. R Core Team. *R: A Language and Environment for Statistical Computing*; R Foundation for Statistical Computing: Vienna, Austria, 2023. Available online: https://www.R-project.org (accessed on 30 October 2023).
41. Rinn, F.; Schweingruber, F.-H.; Schär, E. Resistograph and X-Ray density charts of wood. *Comp. Eval. Drill Resist. Profiles X-ray Density Charts Differ. Wood Species. Holzforsch.* **1996**, *50*, 303–311. [CrossRef]
42. Segundinho, P.G.A.; Silva, A.C.; Gonçalves, F.G.; Regazzi, A.J. Caracterização da madeira laminada colada de *Eucalyptus* sp. produzida com adesivos resorcinol-fenol-formaldeído e poliuretano. *Ciência Da Madeira* **2018**, *9*, 123–133. [CrossRef]
43. Leggate, W.; Shirmohammadi, M.; McGavin, R.L.; Outhwaite, A.; Knackstedt, M.; Brookhouse, M. Examination of wood adhesive bonds via MicroCT: The influence of pre-gluing surface machining treatments for southern pine, spotted gum, and Darwin stringybark timbers. *BioResources* **2021**, *16*, 5058–5082. [CrossRef]
44. Leggate, W.; McGavin, R.L.; Outhwaite, A.; Gilbert, B.P.; Gunalan, S. Barriers to the Effective Adhesion of High-Density Hardwood Timbers for Glue-Laminated Beams in Australia. *Forests* **2022**, *13*, 1038. [CrossRef]
45. Singh, A.K.; Mehra, D.S.; Niyogi, U.K.; Sabharwal, S.; Swiderska, J.; Czech, Z.; Khandal, R.K. Effect of crosslinkers on adhesion properties of electron beam curable polyurethane pressure sensitive adhesive. *Int. J. Adhes. Adhes.* **2013**, *41*, 73–79. [CrossRef]
46. Clauß, S.; Joscak, M.; Niemz, P. Thermal stability of glued wood joints measured by shear tests. *Eur. J. Wood Wood Prod.* **2011**, *69*, 101–111. [CrossRef]
47. Frihart, C. Wood Adhesion and Adhesives. In *Handbook of Wood Chemistry and Wood Composites*, 2nd ed.; CRC Press: Boca Raton, FL, USA, 2012; pp. 255–320.